This is an *Accepted Manuscript*, which has been through the Royal Society of Chemistry peer review process and has been accepted for publication.

Accepted Manuscripts are published online shortly after acceptance, before technical editing, formatting and proof reading. Using this free service, authors can make their results available to the community, in citable form, before we publish the edited article. We will replace this *Accepted Manuscript* with the edited and formatted *Advance Article* as soon as it is available.

You can find more information about *Accepted Manuscripts* in the **Information for Authors**.

Please note that technical editing may introduce minor changes to the text and/or graphics, which may alter content. The journal's standard **Terms & Conditions** and the **Ethical guidelines** still apply. In no event shall the Royal Society of Chemistry be held responsible for any errors or omissions in this *Accepted Manuscript* or any consequences arising from the use of any information it contains.

Journal Name

ARTICLE

The biomolecular corona of nanoparticles in circulating biological media

D. Pozzi,[a,b] G. Caracciolo,[a*] L. Digiacomo,[c,a] V. Colapicchioni,[d] S. Palchetti,[a] A. L. Capriotti,[e] C. Cavaliere,[e] R. Zenezini Chiozzi,[e] A. Puglisi,[e] and A. Laganà[e]

When nanoparticles enter in contact with biological media, they are covered by a biomolecular 'corona', which confers a new identity to the particles. In all the studies reported so far nanoparticles are incubated with isolated plasma or serum that are used as a model for protein adsorption. Anyway, bodily fluids are dynamic in nature so the question arises on whether the incubation protocol, i.e. dynamic vs. static incubation, could affect the composition and structure of the biomolecular corona. Here we let multicomponent liposomes interact with fetal bovine serum (FBS) both statically and dynamically, i.e. in contact with circulating FBS ($\approx$ 40 cm/s). The structure and composition of the liposome–protein corona, as determined by dynamic light scattering, electrophoretic light scattering and liquid chromatography tandem mass spectrometry, were found to be dependent on the incubation protocol. Specifically, following dynamic exposure to FBS, multicomponent liposomes were less enriched in complement proteins and appreciably more enriched in apolipoproteins and acute phase proteins (e.g. Alpha-1-antitrypsin and Inter-alpha-trypsin inhibitor heavy chain H3) that are involved in relevant interactions between nanoparticles and living systems. Supported by our results, we speculate that efficient predictive modeling of nanoparticles behavior *in vivo* will require accurate knowledge of nanoparticle-specific protein fingerprints in circulating biological media.

Introduction

In living systems nanoparticles adsorb biomolecules to form a biomolecular 'corona', which is sufficiently long-lived to confer a new biological identity to the particles.[1, 2] The interactions between living systems and nanoparticles are mediated by this nanoparticle–biomolecule complex rather than the pristine surface. The biomolecular corona around nanoparticles dramatically alters their blood circulation, biodistribution, targeting ability and intracellular fate.[3, 4] Notably, post-translational modification of proteins can affect nanoparticle–cell interactions by adjusting the corona properties.[5] Recently, structure–activity relationships (SARs) have been successfully developed based on corona proteins and many other physic-chemical properties of the nanoparticle-corona as descriptors.[6-8] Few doubt, therefore, that controlling the interaction of nanoparticles with biological systems will require a full description of the corona composition and structure. The biomolecular coronas incorporate several classes of biomolecules with proteins being the most studied.[9] The protein composition of the nanoparticle–corona is dependent on many factors that can be categorized in three main streams: 1) the physicochemical properties of the particles, such as size,[10] shape,[11] and surface properties,[2] 2) the characteristics of

biological media including protein concentration,[12, 13] protein source[14] and temperature[15] and 3) the exposure time that has been identified as a key factor shaping the nanoparticle-corona.[9, 16, 17] In particular, corona composition changes considerably in time due to continuous protein binding and unbinding events up to when final equilibrium is reached typically within a few hours.[9, 16, 17] Irrespective of the nanoparticles properties, biological media and exposure time used, there is bottleneck of precision when mimicking physiological environments. In most studies nanoparticles are incubated with isolated plasma or serum that are used as a model for blood protein adsorption. All these studies, in general, failed to recognize that bodily fluids are highly dynamic in nature. In particular, in the human blood system, flow velocities in the ascending aorta can reach up to 60 cm s^{-1}. One concern is whether the biomolecular corona of nanoparticles formed under static incubation can actually predict that formed *in vivo* thus potentially yielding a partially true pattern of nanoparticle distribution. This mismatch makes correlating *in vitro* data and *in vivo* prediction potentially problematic. We hypothesized that for the very fact that nanoparticles interact with proteins in circulating non-ideal bodily fluids the effect of the flow speed represents a further contribution to the particle coagulation that would allow for

altered biomolecular coronas to form. Here we compared the corona structure formed under static versus dynamic conditions (Figure 1). None of the studies performed so far has compared the corona structure formed under static versus dynamic conditions. To the authors' knowledge, quantitative study of this key issue is new and is addressed in this paper for the first time. Supported by our results, we speculated that the knowledge of nanoparticle-specific protein fingerprints in circulating biological media is required to understand fully the interaction of nanoparticles with biological systems. This understanding is a fundamental issue in hopes of bringing nanotechnology a step closer toward clinical reality.
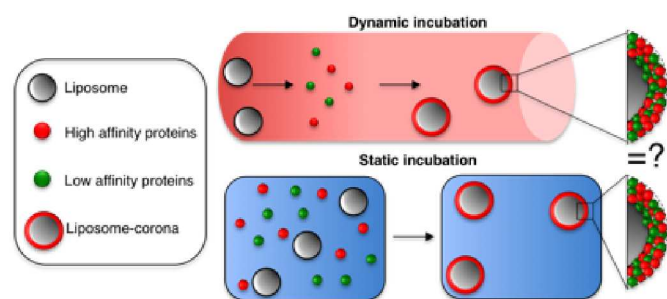
Figure 1. When liposomes come into contact with a biological fluid, a biomolecular layer that is mainly made of proteins covers them. A fundamental question needs to be answered: are the biomolecular coronas formed under dynamic vs. static conditions equal to each other? This is a major challenge towards bringing these nanomaterials from preclinical studies to the clinic.

Results and Discussion

Size and z-potential of liposome-protein corona

To date, liposomes are under extensive investigation as drug delivery systems,[18] with more than 12 drugs in routine clinical use. Following introduction in the bloodstream, liposomes are instantly surrounded by high concentrations of free biomolecules, especially plasma proteins that bind to the liposome surface either due to an advantageous increase in entropy or a decrease in enthalpy. It has been known for decades that proteins interact with nanoparticles *in vivo*, but Dawson et al.[10, 11, 19, 20] were the first to introduce the concept of corona as biomolecular coverage with a composition that evolves over time. The current hypothesis is that liposomes are surrounded by a 'hard protein corona' highly dynamic in nature.[18] The transient liposome–protein corona plays a key role in the bio-nano-interactions being the interface that is "seen" and "processed" by the living organism. The composition of the protein corona is mainly affected the physicochemical properties of the nanoparticle. Nonetheless, other factors such as the temperature,[15] the protein concentration,[12, 13] and the incubation time[9, 17, 21] co-determine its composition and temporal evolution. The biomolecular corona can also change with the animal source (e.g. mouse plasma (MP) vs. human plasma (HP) etc.)[14], the protein source (e.g., serum vs. plasma) and the existence of a disease[22, 23]. While all these factors shaping the biomolecular corona have been deeply explored, whether and how alterations in the

dynamics of the incubation media affect the protein corona has not been investigated so far. In principle, changes in flow velocity patterns as those "experienced" by nanoparticles (NPs) in the body could determine systematic changes in the NP-corona, which could lead, in turn, to different physiological responses. Hence, we investigated size, charge and corona composition of multicomponent (MC) liposomes after incubation with fetal bovine serum (FBS) under static versus dynamic conditions. MC liposomes demonstrated superior efficacy and lower toxicity if compared with the most efficient lipid-based systems.[24-27] Thus, the selected model system is relevant for nanobiomedicine and drug delivery applications. Liposome-protein complexes were characterized thoroughly by dynamic light scattering (DLS) and electrophoretic light scattering (ELS) to estimate the mean hydrodynamic diameter, D_H, and the zeta-potential of MC liposomes (Figure 1, panels A and B respectively). Size and zeta-potential distributions were found to be unimodal and centered at $D_H = 143 \pm 5$ nm and zeta-potential $= 34.5 \pm 1.1$ (Figure 2, panels A and B, t=0). DLS analysis of FBS solution exhibited a trimodal DLS distribution, with peaks centered at 8 nm, 30 nm and 250 nm due to typical protein sizes. After 1 min to exposure of FBS, a single peak was detected at $D_H \approx 220$ nm (Figure 2, panel A, t= 1 min), while DLS peaks of FBS were not seen. One minute of incubation with FBS caused the zeta-potential of MC liposomes to invert sign from positive to negative (zeta-potential= - 26 mV). Collectively our data imply that, as soon as liposomes come into contact with FBS, virtually all serum proteins bind to liposome surface forming a rich biomolecular corona. This result is in good agreement with previous findings[17] showing that the total amount of proteins at 1 min of exposure is much higher than those obtained at 30 and 60 min. For 5 min <60 min, three peaks were detected (Figure 2, panel A, t= 5 min). Two of them coincided with those of FBS centered at 8 nm, 30 nm, while the third one was ascribed to liposome-protein complexes. This observation implies that, for 1 min < t < 5 min, proteins with low affinity dissociate from the lipid particle giving rise to appreciable peaks in the DLS distribution. Such dissociation has a minor effect, if any, on the zeta-potential of the liposome-protein corona. We also observe that, starting from t ≈ 15 min, both size and zeta-potential of the liposome-protein corona reached their final plateau values ($D_H \approx 350\text{-}400$ nm, zeta-potential ≈ -27 mV). In Figure 2 panels C and D we show the temporal evolution of size and zeta-potential upon static (blue circles) and dynamic (red circles) incubation in FBS. Notably, the incubation procedure (i.e. static vs. dynamic incubation) had minor effect, if any, on crude size and zeta-potential values. Of note, we observe that upon dynamic incubation complexes reached their size and zeta-potential equilibrium values faster than their counterpart incubated statically in FBS. This observation could indicate that protein association and particle aggregation is boosted by fluid dynamics. According to literature, time evolution of complex size is due to the combined effect of the serum protein adsorption on single nanoparticles and to the clustering process of k > 1 nanoparticle-corona units.
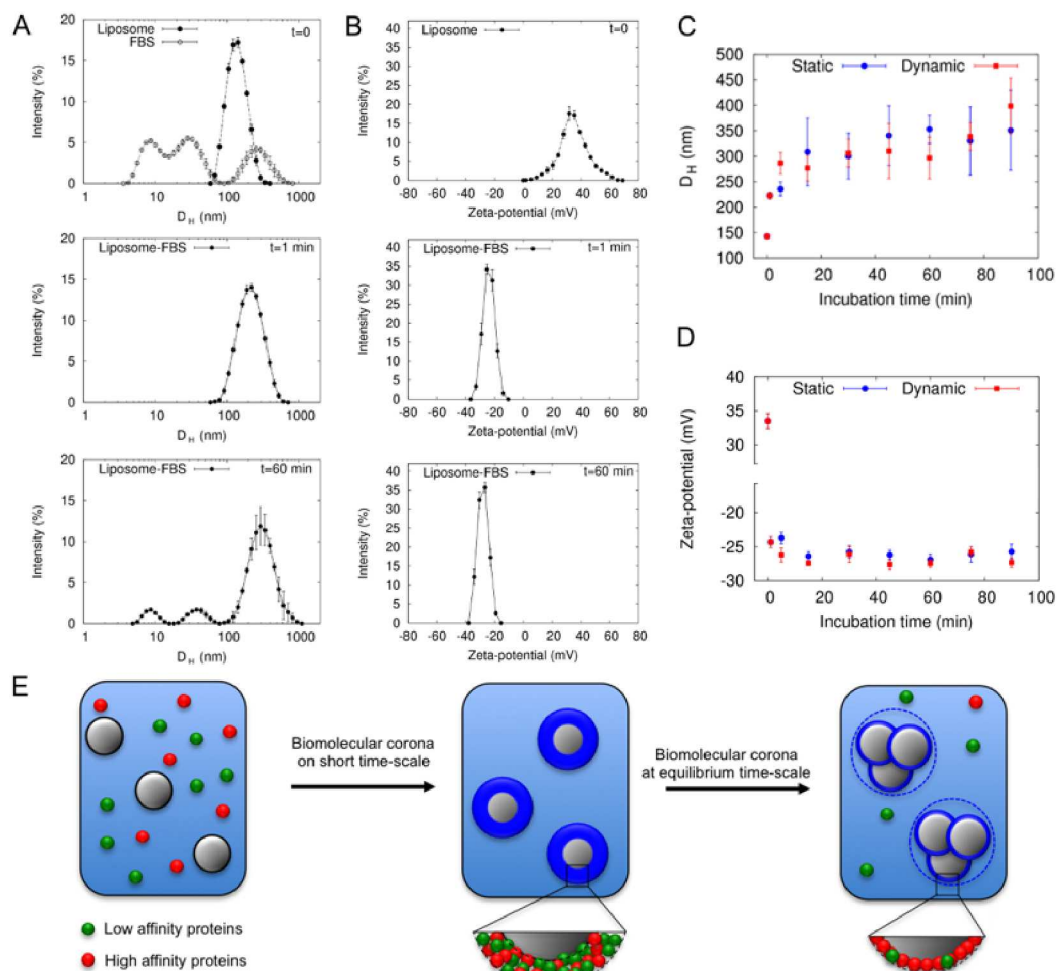
Figure 2. (A) Top panel shows the intensity dynamic light scattering (DLS) distributions of bare liposomes and fetal bovine serum (FBS) (t=0). Middle and bottom panels display intensity of liposome-protein corona at t=1 min and t=60 min respectively. (B) Top panel shows the intensity zeta-potential distributions of bare liposomes (t=0). Middle and bottom panels show zeta-potential distribution of liposome-protein corona at t=1 min and t=60 min respectively. (C) Hydrodynamic diameter (C) and zeta-potential (D) of liposome-protein corona following dynamic (red circles) and static (blue circles) incubation with FBS as a function of the incubation time. (E) Schematic cartoon describing the interaction between liposomes and serum proteins. First, most abundant proteins cover liposomes even if they have low affinity for the liposome surface. On short time-scale (typically 1 minute)[9, 17] DLS and zeta-potential data are compatible with monomers covered by a thick protein corona. With time, larger size aggregates form with low affinity proteins that are substituted by high affinity ones. At equilibrium, aggregates (mostly dimers and trimers)[13, 28] are made of liposomes covered by thinner coronas that likely coexist with monomers (not displayed).

Decoupling these effects is not trivial. However, some general considerations can be made. According to a dense spherical packing model[29] (details can be found in the Electronic Supplementary Information, ESI), the smallest sphere containing two equal rigid spheres of radius r has radius 2r. After 1 minute incubation with FBS, the hydrodynamic diameter of liposome-protein complexes (D_H(t=1 min) ≈ 220 nm) was found to be definitely smaller than double the diameter of bare liposomes (2 D_H(t=0) ≈ 280 nm). As a result, we conclude that on short time-scale (t=1 min) incubation did not produce appreciable particle aggregation. These results are in good agreement with previous findings[17] showing that fast size increase (typically occurring within a few minutes) is mainly due to massive protein adsorption (i.e. single liposomes covered by a thick protein corona). According to this interpretation, we could estimate the thickness of the protein layer as s(1 min) = ½

[D_H(t=1min) - D_H(t=0)] ≈ 40 nm. This thickness is in agreement with those previously reported for other liposome formulations.[14, 30] The biomolecular corona is an extremely flexible layer whose thickness does deeply depend on both the nanoparticle properties and the biological milieu. It can range from a few nanometers for colloidal nanoparticles incubated with single proteins (e.g. human serum albumin[31]) up to 200 nm for PSOSO3 nanoparticles incubated in human plasma for 1 h.[13] By comparing the predicted size-ratios of the spherical packing problem[29] with the hydrodynamic diameter of the liposome-protein complexes (Figure 2, panel C), we deduced that final size of complexes is due to particle agglomeration (a detailed analysis is reported in the ESI). Our data provided a rough estimation of both the number of nanoparticle-corona units in the clusters and the thickness of the protein layer. Aside from being a quantitative determination, we found that equilibrium size of complexes

is compatible with formation of clusters made of up to a few (2-5) nanoparticles each of them covered by thin protein coronas (≈ 6-11 nm). In summary, considering both size evolution and protein dissociation as revealed by DLS, we suggest that smaller size liposome-protein complexes that form on short-time scale (t=1 min) are most likely monomers with thick coronas (≈ 40 nm), while larger size equilibrium complexes (t=1 hour) arise from agglomeration of up to 5 particles covered by thin coronas (≈ 10 nm, Table S1 in the ESI) (a schematic sketch is provided in Figure 2, panel E). These results are in very good agreement with previous findings reported in the literature.[13, 17, 28, 31]

Protein identification and quantification

As above stated, this study is intended as a systematic comparison between the biological identities (size, surface charge, corona composition) of liposomes after interaction with static and circulating FBS. After determining changes in size and zeta-potential we compared the protein coronas formed around MC liposomes in static versus dynamic incubation. We underline that a detailed analysis of the protein composition is not a major aim of this study that is mainly intended as a systematic comparison between the biological identities (size, surface charge and corona composition)[2] of liposomes after interaction with static and circulating FBS. To this end, liquid chromatography tandem mass spectrometry (LC-MS/MS) was applied. LC-MS/MS has great accuracy, high throughput, and more sensitivity and introduces less user bias.[2] Percentage of total protein was determined as explained in the Experimental Section. We identified a total of 334 proteins (Tables S2 and S3). Figure 3 shows the Venn diagram of the total identified proteins, 48 of which exist only after dynamic incubation with FBS, 44 only following static incubation and 242 were in common for both the nanoparticle coronas. Tables S2 and S3 report all the serum proteins bound to MC liposomes following 90 min incubation with FBS under dynamic and static incubation, while Table S4 contains unique proteins (i.e. proteins identified in only one of the two coronas). These results confirm previous studies, where some hundreds of proteins were typically identified in the liposome-corona.[32, 33] Secondly and foremost, we demonstrated that incubating liposomes with FBS under dynamic conditions changed the composition of the biomolecular corona.
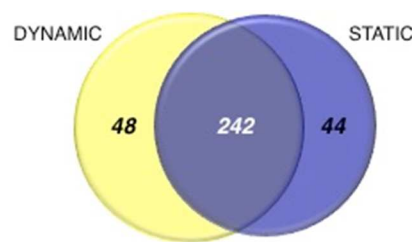
Figure 3. Venn diagram displays the number of proteins identified onto the surface of multicomponent liposomes following dynamic (yellow) and static (blue) incubation with fetal bovine serum. 242 proteins were found in common, while 48 and 44 serum proteins were unique for the single coronas.

Protein classification by molecular mass and charge

According to literature,[9, 34] we categorized all the identified proteins by molecular mass and isoelectric point (pI). As shown in Figure 4A, the incubation protocol let liposomes bind proteins of different molecular weight (MW). Serum proteins with MW < 40 kDa accounted for about 55% of the protein corona. In particular, dynamic incubation promoted extensive binding of proteins with MW < 20 kDa (37 ± 5 %). The incubation protocol significantly impacted the amount of proteins ranging from 100 to 150 kDa whose abundance in the statically formed corona was two-fold (6.8 ± 0.4 %) than its counterpart formed upon dynamic conditions (3.3 ± 0.9 %). Figure 4B displays the protein classification by pI. The largest fraction of corona proteins has a negative charge (pI<7), (about 63.1% and 67.5 % for dynamic and static incubation respectively). Moreover, both formulations adsorb mainly proteins with a pI between 5 and 6 (26.8% and 29.1% following dynamic and static incubation respectively). These results support to the general conception that, in a biological milieu, protein binding to cationic liposomes is mainly driven by electrostatic interactions.[22]

Nonetheless, the charge fingerprints of Figure 4B indicate that, upon dynamic incubation, electrostatic attractions are less important in determining the equilibrium corona structure.

Then, we performed the same analysis on proteins of protein corona, examining the top 25 most abundant proteins that constitute about 70% of the total protein content (Table 1). These proteins have been characterized according to their MW (Figure 4C) and pI (Figure 4D). The same general conclusions we draw for the whole coronas are still valid for the top 25 most abundant proteins. In contrast, we did not find neither serum proteins with MW between 80 and 100 kDa nor proteins with pI>9.

Nanoscale Accepted Manuscript
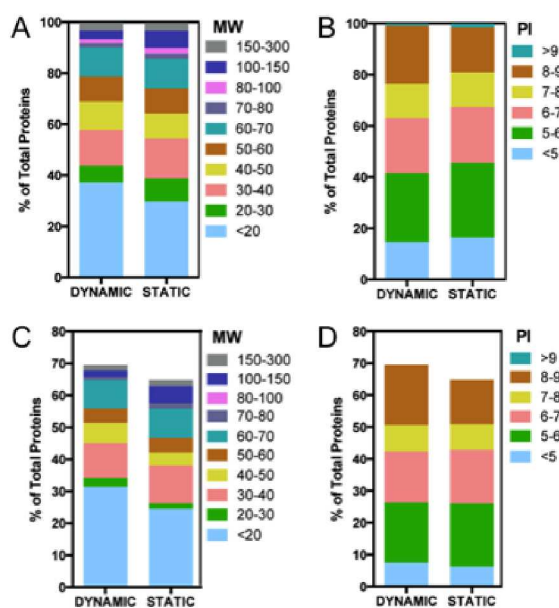
Figure 4. Effect of the incubation protocol on the protein corona composition. (A) Percentage of total protein of corona proteins classified according to their calculated molecular mass and (B) isoelectric point. (C) Percentage of total protein of the top 25 corona proteins classified according to their calculated molecular mass. (D) Percentage of total protein of the top 25 corona proteins categorized according to their isoelectric point. Percentage of total protein was calculated as explained in the Experimental section.

Protein classification by physiological function

Afterwards, the whole identified proteins were categorized according to their physiological function (Figure 5). Of note, percentages of proteins were significantly different between the two coronas. Following 90 min dynamic incubation, the biomolecular corona was less enriched of complement proteins. The main difference regarded CO4, a protein of the classical complement pathway with a known opsonin activity. This result could be relevant for *in vivo* applications, since lower levels of complement proteins are associated to prolonged circulation in the blood. On the other side, the liposome-protein corona was more enriched of lipoproteins (32.4%). The main difference was observed for APOA1 and APOA2 (16.6% and 12.3% for dynamic and static incubation respectively). APOA1 and APOA2 are two of the major protein components of high-density lipoproteins (HDL) in plasma. There are several receptors for apolipoprotein complexes on the cell surfaces, to which liposomes with surface-decorated apolipoproteins can bind. Apolipoproteins may therefore affect the interaction between liposomes and cells with relevance for targeted drug delivery. APOA1-bound cationic liposomes systemically deliver siRNA into mouse hepatocytes expressing Hepatitis C virus (HCV) proteins and inhibit their expression efficiently.[35]

TABLE 1. Top 25 most abundant corona proteins identified in the protein corona of multicomponent liposomes following 90 minutes incubation with fetal bovine serum under dynamic versus static condition. Common proteins are highlighted in gray.

	DYNAMIC			STATIC		
#	Identified Proteins	RPA (%)	St. Dev. (%)	Identified Proteins	RPA (%)	St. Dev. (%)
1	Apolipoprotein A-II	17	2	Apolipoprotein A-II	12.4	0.1
2	Serum albumin	7	1	Serum albumin	6.5	0.4
3	Antitrypsin	5	1	Alpha-2-HS-glycoprotein	5.58	0.07
4	Alpha-2-HS-glycoprotein	5.1	0.6	Hemoglobin fetal subunit beta	4.19	0.07
5	Hemoglobin fetal subunit beta	4.5	0.2	Antitrypsin	4.0	0.2
6	Apolipoprotein C-III	3.7	0.5	Inter-alpha-trypsin inhibitor heavy chain H3	3.7	0.2
7	Apolipoprotein C-II	3.2	0.5	Apolipoprotein C-II	3.5	0.1
8	Apolipoprotein A-I	2.9	0.9	Apolipoprotein C-III	3.32	0.07
9	Hemoglobin subunit beta	2.9	0.2	Alpha-2-macroglobulin	1.98	0.08
10	Hemoglobin subunit alpha	2.3	0.6	Protein AMBP	1.88	0.05
11	Apolipoprotein E	2.05	0.04	Complement C4 (Fragments)	1.73	0.08
12	Alpha-2-macroglobulin	1.75	0.05	Apolipoprotein E	1.7	0.02
13	Clusterin	1.7	0.2	Hemoglobin subunit alpha	1.68	0.04
14	Hyaluronan-binding protein 2	1.5	0.1	Hyaluronan-binding protein 2	1.66	0.09
15	Inter-alpha-trypsin inhibitor heavy chain H3	1.3	0.5	Clusterin	1.63	0.07
16	Apolipoprotein A-IV	0.9	0.3	Apolipoprotein A-I	1.6	0.1
17	Prothrombin	0.88	0.05	Hemoglobin subunit beta	1.2	0.4
18	Apolipoprotein D	0.9	0.1	Lumican	1.03	0.05
19	C4b-binding protein alpha chain	0.84	0.08	C4b-binding protein alpha chain	0.97	0.02
20	Protein AMBP	0.8	0.3	Prothrombin	0.917	0.007
21	Complement C4 (Fragments)	0.8	0.2	Tubulin beta-5 chain	0.78	0.02
22	Tubulin alpha-4A chain	0.74	0.03	Serotransferrin	0.75	0.03
23	Tubulin beta-5 chain	0.71	0.03	Tubulin beta-4B chain	0.746	0.009
24	Tubulin alpha-1B chain	0.70	0.04	Tubulin alpha-4A chain	0.74	0.02
25	Tubulin beta-4B chain	0.69	0.03	Tubulin beta-4A chain	0.699	0.008

A lipid formulation made of dioleoyl-trimethylammonium-propane (DOTAP) and dioleoylphosphatidyletanolamine (DOPE) is able to adsorb onto his surface APOA1 that enables targeted delivery of intracellular-acting protein drugs to nonsmall cell lung tumors for the treatment of lung cancer.[36] After exposure to FBS, percentages of identified acute phase proteins were very similar to each other. Main differences were found for Alpha-1-antitrypsin (A1AT) and Inter-alpha-trypsin inhibitor heavy chain (ITIH3). Both proteins are involved in relevant biological processes. A1AT is inhibitor of serine proteases and an anti-inflammation protein that works as an immune system regulator. It has been reported that A1AT affects lymphocyte proliferation and cytotoxicity and mediates monocyte and neutrophil functions.[37] Due to its role on anti-inflammation the enrichment with A1AT could reduce the attraction of macrophages to the site of nanoparticle accumulation. Nonetheless, A1AT has exhibited anti-apoptotic function for lung microvascular endothelial cells and epithelial cells.[38] ITIH3 may act as a carrier of hyaluronan in serum or as a binding protein between hyaluronan and other matrix proteins. Since hyaluronan is a major component of glycoproteins that are located at the cell plasma membrane and the extracellular matrix, surface-adsorbed hyaloronan-binding proteins may promote the interaction of nanoparticles with the cell surface. Lastly, we observe that the incubation procedure had a minor impact, if any, on the binding of coagulation system proteins, tissue leakage proteins and other proteins (i.e. relevant proteins not included in any of the previous classes) to MC liposome surface.

Experimental

Chemicals

1,2-Dioleoyl-3-trimetylammonium-propane (DOTAP), (3-[N-(N',N'-dimetylaminoethane)-carbamoyl])-cholesterol (DC-Chol), dioleoylphosphocholine (DOPC) and dioleoylphosphatidyletanolamine (DOPE) were purchased from Avanti Polar Lipids (Alabaster, AL). Organic solvents and Fetal Bovine Serum (FBS) were purchased from Sigma-Aldrich (St. Louis, MO, USA). The sequencing grade modified trypsin was purchased from Promega (Madison, WI, USA). Ultrapure water (resistivity 18.2 MΩ cm) was achieved by an Arium water purification system (Sartorius, Florence, Italy).

Multicomponent liposome preparation

Liposomes were prepared in accordance with standard procedures by dissolving appropriate amounts of lipids at φ = neutral lipid/total lipid (mol/mol) = 0.5. Multicomponent (MC) liposomes were synthesized according with these molar ratios DOTAP:DOPC: DCChol: DOPE (1:1:1:1). Lipid films were hydrated (final lipid concentration 1 mg/mL) with PBS 10 mM (pH=7.4) and then
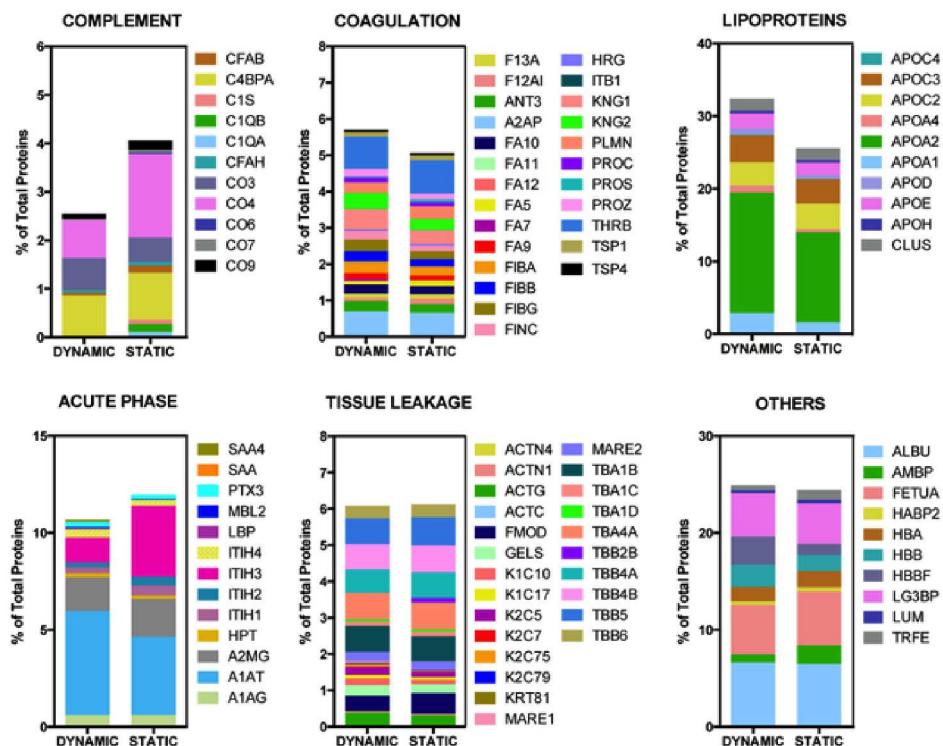
Figure 5. Bioinformatic classification of corona proteins. Percentage of total proteins identified in the corona of multicomponent liposome following 90 min exposure to fetal bovine serum under dynamic vs. static conditions. Detailed values for all individual proteins are available in Supporting Information.

extruded 20 times through a 0.1μm Polycarbonate carbonate filter by the Avanti Mini-Extruder (Avanti Polar Lipids, Alabaster, AL).

Size and zeta-potential measurements

Size and zeta-potential measurements were made on a Zetasizer Nano ZS90 (Malvern, U.K.) at 25 °C. Bare liposomes were diluted 1:100 with PBS 10mM. Results are given as mean ± standard deviation of five replicates.

Static incubation

Static incubation experiments were performed by mixing 200 μL of liposome dispersion with 200 μL of freshly clarified FBS. Mixed solutions were incubated for different times at room temperature. To perform size and zeta-potential experiments 20 μL of the liposome:FBS solution were diluted with 980 μL of a solution PBS:H$_2$O (1:80 v/v), in order to obtain a final particle concentration of 10 ng/ml. For proteomics experiments, the experimental procedure was exactly the same, but a 3-fold larger volume of liposome/FBS solution was used (1.8 ml). According to previous findings, [27] this is the minimum sampling volume required for accurate protein identification and quantification by nanoLC-MS/MS.

Dynamic incubation

A peristaltic pump (Watson and Marlow, UK) furnished with silicon tubes (internal diameter 1.6 mm, total length 250 mm) was used to propel liposome:FBS solution. According to the manufacturer's instruction, the rounds per minute (RPM) were adjusted to obtain suitable flow rates. RPM were adjusted to mimic the human abdominal aortic flow velocity ($\approx$ 40 cm/s). For size and zeta-potential experiments, 300 μL of liposome solution (1mg/ml in PBS 10 mM) were mixed with 300 μL of freshly clarified FBS and poured inside the silicon tube by a microfine insulin syringe (Becton, Dickinson and Company, USA). To avoid formation of air bubbles the syringe was let act as a stopper. At different times, 20 μL of the circulating solution were collected from silicon tube by a Hamilton syringe and immediately transferred into the Zetasizer sample holder. For proteomics experiments, the large sampling volume of liposome/FBS solution (1.8 ml) resulted in the use of 820 mm long silicon tubes.

Proteomics experiments

MC liposomes were mixed with FBS (1:1 v/v) and were incubated at RT for 90 min, either for static and dynamic incubation. This volume ratio was chosen because it is mimetic of *in vivo* condition. Volume value was chosen in order to obtain a minimal quantity of protein, according to the procedural showed in.[30] After incubation, the samples were centrifuged 15 min at 14000 rpm followed by pellet resuspension in PBS 10mM; this procedure was repeated three times to wash the sample and remove all the molecules not bound to the MC liposomes. According to literature,[39] all

the aforementioned steps aimed at separating unbound proteins from liposome-protein conjugates are associated with technical hurdles (e.g. technically it is quite difficult to separate 100% of the supernatant) and may lead to possible bias. In addition, each repetitive centrifugation step does modify the equilibrium of the protein corona with the result that the final corona does not reflect the original situation. This is something to keep in mind to achieve quantitative and comparable data.[39] Anyway, the main aim of this work was not the most accurate possible determination of the protein corona composition, but the demonstration that the nature of the incubation process (i.e. static vs. dynamic incubation) can affect the final corona composition. Even though all the needed purification steps could change the original protein corona composition, different final protein corona compositions, as those we observed after static vs. dynamic incubations, were no doubt due to differences in the original compositions (i.e. before purification steps).

In solution digestion and desalting

The protein pellets obtained from precipitation were resuspended in 50 μL of a denaturant buffer composed of 8 mol L^{-1} urea in 50 mmol L^{-1} NH4HCO3, then 2.5 μL of DTT 200 mmol L^{-1} in 50 mmol L-1 NH4HCO3 were added and finally incubated for 1 h at 37 °C. Following protocols already described,[28] the protein extract was enzymatically digested before nanoLC-MS/MS analysis. After overnight digestion at 37 °C, the reaction was quenched by the addition of HCOOH. Digested samples were desalted using an SPE C18 column (Bond Elut 1CC LRCC18,Varian, Palo Alto, CA, USA). Peptides were eluted from the SPE column with 0.5 mL ACN: H2O (50:50, v/v) solution containing 0.05% TFA and were vacuum dried. Each sample was reconstituted with 300 μL of a 0.1% HCOOH solution. Digested samples were stored at -80°C until nanoLC-MS/MS analysis.

NanoLC-MS/MS analysis

Tryptic peptides were analyzed using a Dionex Ultimate 3000 (Sunnyvale, CA, USA) nanoLC system connected to the hybrid mass spectrometer Orbitrap Elite (Thermo Fisher Scientic Bremen, Germany), equipped with a nanoelectrospray ion source. Peptide mixtures were enriched by injecting 10 μL of sample on line, onto a 300 μm i.d. x 5 mm Acclaim PepMap 100 C18(5 μm particle size, 100 Å pore size) μ-precolumn (Dionex), using a premixed mobile phase H2O/ACN 98:2 (v/v) containing 0.1% TFA at 10 μL min flow-rate. Peptide mixtures were separated by reversed-phase chromatography on in-house manufactured 25 cm fritless silica microcolumns with a 75 μm i. d. The column was packed with ReproSil-Pur C18-AQ 2.2 μm resin (Dr. Maisch GmbH, Ammerbuch, Germany). Mobile phase was H2O (A) and ACN (B), both with 0.1% (v/v) HCOOH. After a 5 min isocratic step at 5%, B was led to 10% in 2 min. Then, B was linearly increased from 10% to 25% within 100 min and then to 55% in 43 min. After that, B was

increased to 80%within 5 min and kept constant for 20 min. Then, B was dcreased to 1% and within 1 min and kept constant for the following 44 min to rinse the column (220 min total run time). MS spectra were collected over an m/z range of 380-2000 at 60000 resolution, operating in the data dependent mode to switch automatically between Orbitrap-MS and Ion Trap-MS/MS acquisition. Following "TOP20 strategy", MS/MS spectra were collected for the twenty most intense ions with a charge state greater than 1, using a dynamic exclusion of 60 s. CID was performed with normalized collision energy set at 30%. All samples were analyzed in triplicate in order to assess the additional variation introduced in the measurements by the experimental procedure and to increase the number of identified proteins.

Data analysis and protein validation

Raw data files, obtained from Xcalibur software, were submitted to Proteome Discover (1.2 version, Thermo Scientific) for database search using Mascot (version 2.3.2 Matrix Science). Data were searched against SwissProt database (57.15 version, 20266 sequences). The built-in decoy search option of Mascot was used. Enzymatic digestion with trypsin was selected, along with maximum 2 missed cleavages, peptide charges +2 and +3, a 10 ppm precursor mass tolerance and 0.8 Da fragment mass tolerance; acetylation (N-term), oxidation (M) and deamidation (N, Q) were used as dynamic modifications; carbamidomethylation (C) was used as static modification. The Scaffold software (version 3.1.2, Proteome Software Inc.) was used to validate MS/MS-based peptide and protein identifications and for label-free relative quantitation based on spectral counting. The peptide and protein probabilities were set to minimum 95% and 99%, respectively, with at least one identified peptide. For protein quantitative analysis, Scaffold software allows the normalization of the spectral countings (normalized spectral countings, NSCs) and offers various statistical tests to identify significant abundance differences in two or more categories. The mean value of NSCs obtained in the three experimental replicates for each protein was further normalized to the protein molecular weight (MWNSC) and expressed as the relative protein quantity by applying the following equation:

$$MWNSC_k = \frac{(NSC/MW)_k}{\sum_{i=1}^{N}(NSC/MW)_i} \times 100 \qquad (1)$$

where $MWNSC_k$ is the percentage molecular weight normalized NSC for protein k, and MW is the molecular weight in kDa for protein k. This correction takes into account the protein size and evaluates the actual contribution of each protein reflecting its percentage, i.e the relative protein abundance (RPA) in the 'hard corona'.

Conclusion

In summary, the biomolecular corona that forms around nanoparticles in circulating biological media might be different from its counterpart formed under static conditions, i.e. the only experimental condition used so far. Given the strict relationship between the biological identities that nanoparticles acquire *in vivo* and their physiological response (blood circulation times, immune response, selective targeting, etc.) our results suggest the need for a re-evaluation of how prediction studies should be planned in the future and how *in vitro-in vivo* extrapolations can be made. The protein corona composition formed under proper dynamic condition is likely the most accurate descriptor for QSARs to be done. We speculate that the corona composition could be affected also by differential flow velocity. In a blood vessel, as in any non-ideal fluid, the speed of the fluid at the boundary (relative to the boundary), and therefore that of the nanoparticle, is zero, while the flow speed acquires its maximum value along the axis of the blood vessel. Nonetheless, since blood vessels of diverse size (e.g. arterial vs. tumor blood vessels) differ in flow rates by orders of magnitude, this would imply that the biomolecular corona, and therefore the nanoparticle biological identity, could dynamically change as a function of its localization in the body. Among technical hurdles, rapid extraction of nanoparticles from silicon tubes could be a major concern. Indeed, even if we filled centrifugation tubes with the extracted circulating fluid very fast, equilibrium of the protein corona could change, although minimally, during extraction with the result that the protein corona could not exactly reflect the original situation. In addition, here we incubated liposomes with isolated HP that was used as a model for blood protein adsorption. However, the non-Newtonian fluid dynamics of blood and plasma are different from each other so that the incubation in blood may lead to substantial changes of the present results as compared to those obtained using HP. Nowadays, it is emerging the idea that accurate prediction of the nanoparticles outcome *in vivo* will need not only the knowledge of the corona composition but also mapping protein binding sites on the nanoparticle-protein corona.[40] Altogether, understanding the effect of the incubation procedure on the location of protein binding sites on the biomolecular corona is a compelling task for future research. Thus, we believe that many other relevant perspectives of research will emerge from the results of this work.

Acknowledgements

Nanoscale Accepted Manuscript

Notes and references

ᵃDepartment of Molecular Medicine, "Sapienza" University of Rome, Viale Regina Elena 291, 00161 Rome, Italy

ᵇIstituti Fisioterapici Ospitalieri,) Istituto Regina Elena,) Via Elio Chianesi 53, 00144 Rome, Italy

ᶜDepartment of Bioscience and Biotechnology, University of Camerino, Via Gentile III da Varano, Camerino (MC), 62032, Italy

ᵈIstituto Italiano di Tecnologia, Center for Life Nano Science@Sapienza, Viale Regina Elena 291, 00161, Rome, Italy

ᵉDepartment of Chemistry, "Sapienza" University of Rome, P.le A. Moro 5, 00185 Rome, Italy

***E-mail: giulio.caracciolo@uniroma1.it

1. M. P. Monopoli, C. Åberg, A. Salvati and K. A. Dawson, *Nature nanotechnology*, 2012, **7**, 779-786.
2. C. D. Walkey and W. C. W. Chan, *Chemical Society Reviews*, 2012, **41**, 2780-2799.
3. K. Hamad-Schifferli, *Nanomedicine*, 2015, **10**, 1663-1674.
4. L. Treuel, D. Docter, M. Maskos and R. H. Stauber, *Beilstein journal of nanotechnology*, 2015, **6**, 857-873.
5. S. Wan, P. M. Kelly, E. Mahon, H. Stöckmann, F. Caruso, K. A. Dawson, Y. Yan and M. P. Monopoli, *ACS nano*, 2015.
6. R. Liu, W. Jiang, C. D. Walkey, W. C. Chan and Y. Cohen, *Nanoscale*, 2015, **7**, 9664-9675.
7. C. D. Walkey, J. B. Olsen, F. Song, R. Liu, H. Guo, D. W. H. Olsen, Y. Cohen, A. Emili and W. C. Chan, *ACS nano*, 2014, **8**, 2439-2455.
8. P. Kamath, A. Fernandez, F. Giralt and R. Rallo, *Current topics in medicinal chemistry*, 2015.
9. S. Tenzer, D. Docter, J. Kuharev, A. Musyanovych, V. Fetz, R. Hecht, F. Schlenk, D. Fischer, K. Kiouptsi and C. Reinhardt, *Nature nanotechnology*, 2013, **8**, 772-781.
10. T. Cedervall, I. Lynch, S. Lindman, T. Berggård, E. Thulin, H. Nilsson, K. A. Dawson and S. Linse, *Proceedings of the National Academy of Sciences*, 2007, **104**, 2050-2055.
11. T. Cedervall, I. Lynch, M. Foy, T. Berggård, S. C. Donnelly, G. Cagney, S. Linse and K. A. Dawson, *Angewandte Chemie International Edition*, 2007, **46**, 5754-5756.
12. G. Caracciolo, D. Pozzi, A. L. Capriotti, C. Cavaliere, P. Foglia, H. Amenitsch and A. Laganà, *Langmuir*, 2011, **27**, 15048-15053.
13. M. P. Monopoli, D. Walczyk, A. Campbell, G. Elia, I. Lynch, F. Baldelli Bombelli and K. A. Dawson, *Journal of the American Chemical Society*, 2011, **133**, 2525-2534.
14. G. Caracciolo, D. Pozzi, A. L. Capriotti, C. Cavaliere, S. Piovesana, G. La Barbera, A. Amici and A. Laganà, *Journal of Materials Chemistry B*, 2014, **2**, 7419-7428.
15. M. Mahmoudi, A. M. Abdelmonem, S. Behzadi, J. H. Clement, S. Dutz, M. R. Ejtehadi, R. Hartmann, K. Kantner, U. Linne and P. Maffre, *ACS nano*, 2013, **7**, 6555-6562.
16. M. Lundqvist, J. Stigler, T. Cedervall, T. Berggård, M. B. Flanagan, I. Lynch, G. Elia and K. Dawson, *ACS nano*, 2011, **5**, 7503-7509.
17. A. L. Barrán-Berdón, D. Pozzi, G. Caracciolo, A. L. Capriotti, G. Caruso, C. Cavaliere, A. Riccioli, S. Palchetti and A. Laganaì, *Langmuir*, 2013, **29**, 6485-6494.
18. G. Caracciolo, *Nanomedicine: Nanotechnology, Biology and Medicine*, **11**, 543-557.
19. M. Lundqvist, J. Stigler, G. Elia, I. Lynch, T. Cedervall and K. A. Dawson, *Proceedings of the National Academy of Sciences*, 2008, **105**, 14265-14270.
20. I. Lynch and K. A. Dawson, *Nano Today*, 2008, **3**, 40-47.
21. M. Lundqvist, *Nature nanotechnology*, 2013, **8**, 701-702.
22. M. J. Hajipour, S. Laurent, A. Aghaie, F. Rezaee and M. Mahmoudi, *Biomaterials Science*, 2014, **2**, 1210-1221.
23. A. A. Saie, M. Ray, M. Mahmoudi and V. M. Rotello, in *Nanotechnology-Based Precision Tools for the Detection and Treatment of Cancer*, Springer, 2015, pp. 245-273.
24. G. Caracciolo, D. Pozzi, R. Caminiti, C. Marchini, M. Montani, A. Amici and H. Amenitsch, *Biochimica et Biophysica Acta - Biomembranes*, 2007, **1768**, 2280-2292.
25. G. Caracciolo, D. Pozzi, R. Caminiti, C. Marchini, M. Montani, A. Amici and H. Amenitsch, *Journal of Physical Chemistry B*, 2008, **112**, 11298-11304.
26. D. Pozzi, C. Marchini, F. Cardarelli, A. Rossetta, V. Colapicchioni, A. Amici, M. Montani, S. Motta, P. Brocca and L. Cantù, *Molecular pharmaceutics*, 2013, **10**, 4654-4665.
27. D. Pozzi, C. Marchini, F. Cardarelli, F. Salomone, S. Coppola, M. Montani, M. E. Zabaleta, M. Digman, E. Gratton and V. Colapicchioni, *Biochimica et Biophysica Acta (BBA)-Biomembranes*, 2014, **1838**, 957-967.
28. G. Caracciolo, F. Cardarelli, D. Pozzi, F. Salomone, G. Maccari, G. Bardi, A. L. Capriotti, C. Cavaliere, M. Papi and A. Laganà, *ACS applied materials & interfaces*, 2013, **5**, 13171-13179.
29. R. M'Hallah, A. Alkandari and N. Mladenovic, *Computers & Operations Research*, 2013, **40**, 603-615.
30. D. Pozzi, V. Colapicchioni, G. Caracciolo, S. Piovesana, A. L. Capriotti, S. Palchetti, S. De Grossi, A. Riccioli, H. Amenitsch and A. Lagana, *Nanoscale*, 2014, **6**, 2782-2792.
31. C. Röcker, M. Pötzl, F. Zhang, W. J. Parak and G. U. Nienhaus, *Nature nanotechnology*, 2009, **4**, 577-580.
32. D. Pozzi, V. Colapicchioni, G. Caracciolo, S. Piovesana, A. L. Capriotti, S. Palchetti, S. De Grossi, A. Riccioli, H. Amenitsch and A. Lagana, *Nanoscale*, 2014, **6**, 2782-2792.
33. S. Tenzer, D. Docter, J. Kuharev, A. Musyanovych, V. Fetz, R. Hecht, F. Schlenk, D. Fischer, K. Kiouptsi, C. Reinhardt, K. Landfester, H. Schild, M. Maskos, S. K. Knauer and R. H. Stauber, *Nature nanotechnology*, 2013, **8**, 772-781.
34. D. Pozzi, G. Caracciolo, A. L. Capriotti, C. Cavaliere, G. La Barbera, T. J. Anchordoquy and A. Laganà, *Journal of proteomics*, 2015, **119**, 209-217.
35. S. I. Kim, D. Shin, H. Lee, B.-Y. Ahn, Y. Yoon and M. Kim, *Journal of hepatology*, 2009, **50**, 479-488.
36. S. K. Kim, M. B. Foote and L. Huang, *Biomaterials*, 2012, **33**, 3959-3966.
37. N. Pirooznia, S. Hasannia, A. S. Lotfi and M. Ghanei, *J Nanobiotechnology*, 2012, **10**, 20-35.
38. S. Sohrab, D. N. Petrusca, A. D. Lockett, K. S. Schweitzer, N. I. Rush, Y. Gu, K. Kamocki, J. Garrison and I. Petrache, *The FASEB Journal*, 2009, **23**, 3149-3158.
39. P. Del Pino, B. Pelaz, Q. Zhang, P. Maffre, G. U. Nienhaus and W. J. Parak, *Materials Horizons*, 2014, **1**, 301-313.
40. P. M. Kelly, C. Åberg, E. Polo, A. O'Connell, J. Cookman, J. Fallon, Ž. Krpetić and K. A. Dawson, *Nature nanotechnology*, 2015.